

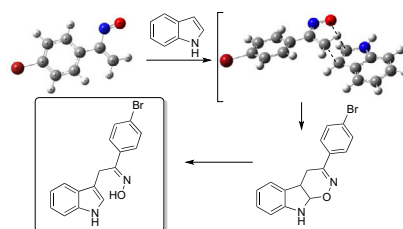
Reactivity of 1-arylnitrosoethylenes towards indole derivatives

Susana M. M. Lopes¹ · Sandra C. C. Nunes¹ · Cátia C. Caratão¹ ·
Alberto A. C. C. Pais¹ · Teresa M. V. D. Pinho e Melo¹

Received: 2 February 2016 / Accepted: 17 April 2016 / Published online: 7 June 2016
© Springer-Verlag Wien 2016

Abstract The reactivity of 1-arylnitrosoalkenes toward indole, 1-methylindole, and 3-methylindole is described. In contrast with the previously observed chemical behaviour of 1-(*p*-bromophenyl)nitrosoethylene towards pyrrole, the studied heterodienes reacted with indole and 1-methylindole to afford *E*-oximes via hetero-Diels–Alder reactions. The reaction with 3-methylindole also proceeds via cycloaddition giving the corresponding 1,2-oxazine. Quantum chemical calculations, at the DFT level, indicate that the energy barriers associated with the reactions between 1-(*p*-bromophenyl)nitrosoethylene and indole and its derivatives are similar to those observed for the reaction between this nitrosoalkene and pyrrole. However, the calculated energy of the theoretical Diels–Alder cycloadducts involving indole and pyrrole clearly suggests that the Diels–Alder reaction is privileged in the case of indole. Furthermore, in the case of the indole, the energy difference between reactants and products clearly favors the regiochemistry observed experimentally.

Graphical abstract



Keywords Diels–Alder reaction · Nitrosoalkenes · Indoles · DFT calculations

Introduction

It is generally accepted that Diels–Alder cycloadditions between asymmetrically substituted dienes or heterodienes and/or asymmetrically substituted dienophiles take place through highly asymmetric transition state structures. These reactions are characterized by an asynchronous bond formation, a process initiated by the formation of the first α -bond between the most electrophilic and nucleophilic centers of the reagents with concomitant ring-closure. This is the case of the reaction of conjugated nitrosoalkenes, generated in situ by base-mediated dehydrobromination of α -bromooximes, with electron rich olefins which has been explored as a general route to oxazines, the expected Diels–Alder cycloadducts [1–3]. On the other hand, nitrosoalkenes **2a** and **2b** are known to react with electron rich heterocycles such as pyrrole and indole to give open chain oximes resulting from rearomatization of the pyrrole unit of the initially formed Diels–Alder cycloadducts.

Electronic supplementary material The online version of this article (doi:10.1007/s00706-016-1763-1) contains supplementary material, which is available to authorized users.

✉ Teresa M. V. D. Pinho e Melo
tmelo@ci.uc.pt

¹ CQC and Department of Chemistry, University of Coimbra, 3004-535 Coimbra, Portugal

Oximes **4** were isolated as single stereoisomers, the expected outcome for the ring-opening reaction of bicyclic 1,2-oxazines (Scheme 1) [4–6].

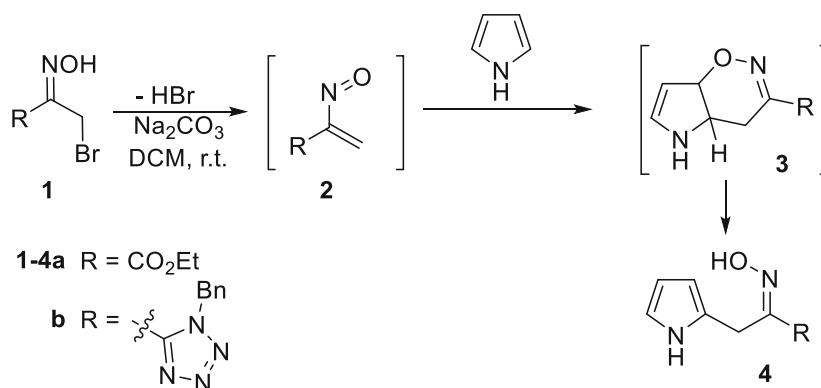
However, we have recently demonstrated that 1-(*p*-bromophenyl)nitrosoethylene (**5a**) show a different chemical behaviour towards pyrrole (Scheme 2) [7]. Two isomeric oximes are formed which cannot be explained by a process involving hetero-Diels–Alder reaction. Instead, the synthesis of the 2-alkylated pyrroles **7** and **9** results from a conjugate addition followed by a 1,5-sigmatropic hydrogen-shift. Starting from nitrosoalkene **5a** at the *s-cis* conformation oxime **7** is obtained whereas **5a-s-trans** affords oxime **9**. Quantum chemical calculations, at the DFT level of theory, predict that the Diels–Alder reaction of pyrrole is favoured in the case of ethyl nitrosoacrylate (**2a**) and point to a different reaction pathway for 1-(*p*-bromophenyl)nitrosoethylene (**5a**), corroborating the experimental findings. In fact, the results demonstrate that the barriers associated with the reactions involving

nitrosoalkene **5a** and pyrrole is over 30 kJ/mol higher than the one involving ethyl 2-nitrosoacrylate (**2a**).

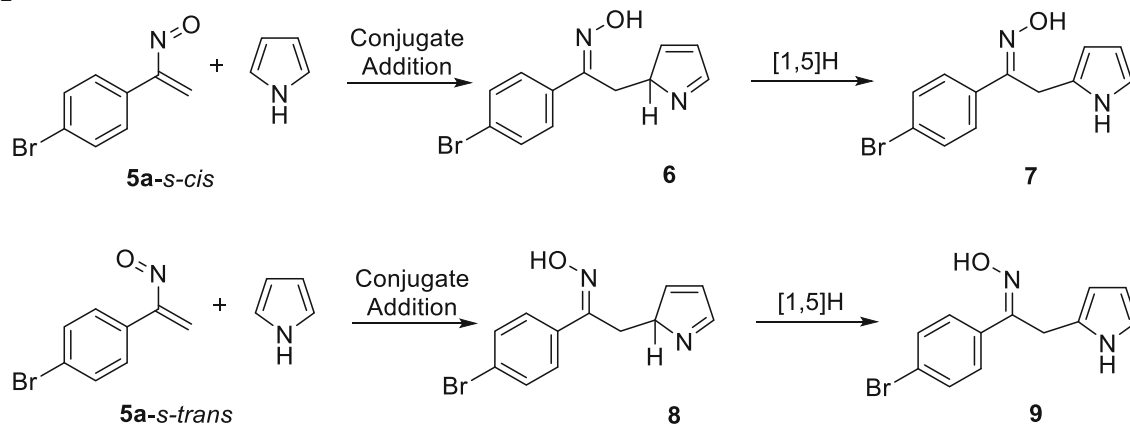
This unexpected reactivity of 1-(*p*-bromophenyl)nitrosoethylene (**5a**) led us to become interested on the study of the chemical behaviour of this nitrosoalkene towards indole derivatives. Indole undergoes alkylation at the 3-position on reacting with ethyl 2-nitrosoacrylate (**2a**) and 1-benzyl-5-(1-nitrosovinyl)-1*H*-tetrazole (**2b**). Indoles **10** were isolated as single stereoisomer, the expected outcome for the ring-opening reaction of the corresponding cycloadducts. Evidence for the generation of the nitrosoalkenes **2** followed by Diels–Alder reaction also comes from the reaction of α -bromooximes **1** with 3-methylindole to give 1,2-oxazines **11** (Scheme 3) [4–6].

We set out to explore the generation and reactivity of 1-arylnitrosoethylenes in the presence of indole derivatives since it could give new insight into the chemistry of conjugated nitrosoalkenes.

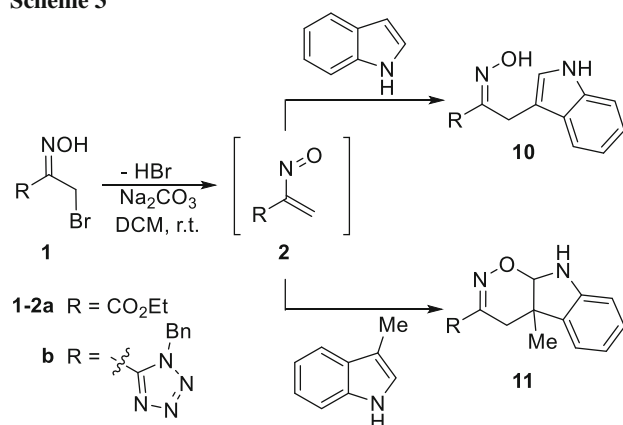
Scheme 1



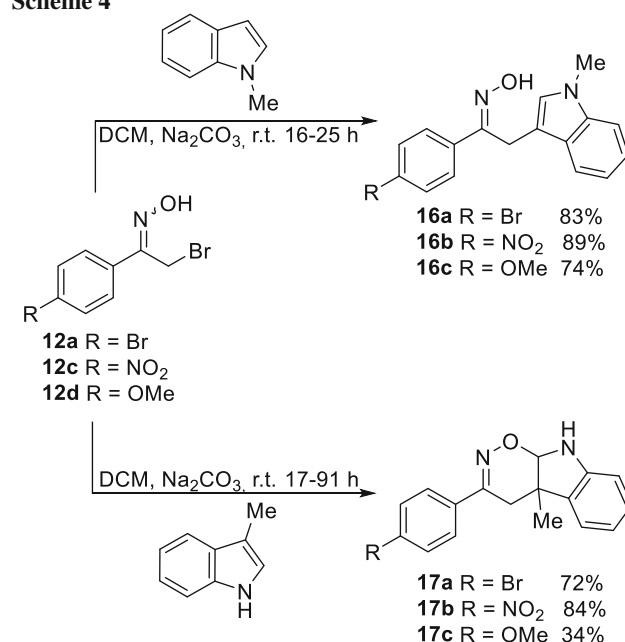
Scheme 2



Scheme 3



Scheme 4



Results and discussion

The reaction of 1-(*p*-bromophenyl)nitrosoethylene (**5a**) and phenylnitrosoethylene (**5b**) with indole was studied (Table 1). The dehydrobromination of 1-(*p*-bromophenyl)ethanone oxime (**12a**) was carried out at room temperature in dichloromethane using sodium carbonate as base and in the presence of indole affording oxime **13a** and two *N*-alkylated derivatives **14a** and **15a** in 64 % overall yield (Table 1, entry 1). A similar outcome was observed when nitrosoalkene **5b**, generated from **12b** under the same reaction conditions, reacted with indole (Table 1, entry 2). It is noteworthy that oximes **13** were isolated as single stereoisomers, which were assigned as *anti* isomers based on NMR data. The isomeric compounds **14** and **15** are formed by *N*-alkylation of compounds **13**.

The formation of compounds **14** and **15** was unexpected since the reaction of nitrosoalkenes with indole usually does not lead to *N*-alkylated products (see Scheme 3). However, *N*-alkylated indoles have been previously observed as products of the reaction of azoalkenes with indole [8, 9].

In order to avoid *N*-alkylation reactions, 1-methylindole was selected as the electron rich heterocycle and the reactivity towards nitrosoalkene **5a** studied. From this reaction oxime **16a** was obtained in 83 % yield, the expected product of a hetero-Diels–Alder reaction. The same reactivity was observed carrying out the reaction of oximes **12c** and **12d** with 1-methylindole affording in good yields indoles **16b** and **16c**, respectively. On the other hand, 3-methylindole reacted with nitrosoalkenes derived from oximes **12a**, **12c**, and **12d** to afford cycloadducts **17**, since the methyl group in 3-position prevents the ring opening reaction (Scheme 4).

Electronic structure calculations were carried out in order to investigate the reactivity of indole and the two derivatives studied towards 1-(*p*-bromophenyl)nitrosoethylene (**5a**). Contrarily to the previously observed

Table 1 Reaction of nitrosoalkenes **5** with indole

Entry	Oxime	Reaction time/h	Products/%
1	12a	17	13a 24 14a 16 15a 24
2	12b	46	13b 27 14b 14 15b 28

Table 2 Energy barriers, ΔE , and asynchronicity, $Async$, of the transition states for the reaction of 1-(*p*-bromophenyl)nitrosoethylene (**5a**) with indole, 1-methylindole, and 3-methylindole, calculated atthe B3LYP/6-31G(d,p) level of theory considering the lower energy conformer of 1-(*p*-bromophenyl)nitrosoethylene

Reaction	TS	$\Delta E/\text{kJ mol}^{-1}$	$d(\text{C}-\text{C})/\text{\AA}$	$d(\text{C}-\text{O})/\text{\AA}$	$Async$
Observed regiochemistry					
Indole	TS _{endo}	67.6	2.09	2.46	0.08
Indole	TS _{exo}	62.1	2.11	2.46	0.08
3MeIndole	TS _{endo}	74.1	2.07	2.45	0.08
3MeIndole	TS _{exo}	72.2	2.11	2.41	0.07
1MeIndole	TS _{endo}	60.3	2.10	2.54	0.09
1MeIndole	TS _{exo}	57.4	2.11	2.51	0.09
Opposite regiochemistry					
Indole	TS _{endo}	76.1	2.05	2.53	0.10
Indole	TS _{exo}	75.3	2.06	2.51	0.10
3MeIndole	TS _{endo}	71.8	2.06	2.68	0.13
3MeIndole	TS _{exo}	75.4	2.03	2.76	0.15
1MeIndole	TS _{endo}	77.5	2.06	2.47	0.09
1MeIndole	TS _{exo}	76.8	2.05	2.52	0.10

ZPE correction and BSSE corrections were taken into account. Asynchronicity was calculated according to $Async = [d(\text{C}-\text{O}) - d(\text{C}-\text{C})] / [d(\text{C}-\text{O}) + d(\text{C}-\text{C})]$. Parameters $d(\text{C}-\text{C})$ and $d(\text{C}-\text{O})$ correspond to the lengths, in the transition-state, of carbon-carbon and carbon-oxygen formed bonds

reactivity of 1-(*p*-bromophenyl)nitrosoethylene towards pyrrole [7], experimental results concerning the reactions between indole, and respective derivatives with the referred nitrosoalkene are compatible with a reaction occurring via Diels–Alder cycloaddition.

The transition state (TS) resulting from the *endo*- and *exo*-cycloadditions of indole and two of its derivatives (1-methylindole and 3-methylindole) with 1-(*p*-bromophenyl)nitrosoethylene were investigated at the DFT level. Calculations were performed using the Gamess program package [10], with graphical representations produced with Molden 5.0.

In each case, full geometry optimizations of the transition structures were performed using the B3LYP hybrid functional [11–13] and the 6-31G(d,p) basis set, followed by harmonic frequency calculations at the same level of theory, which confirmed the nature of the stationary points. The starting structure in each case was derived from the *s-cis* conformer of 1-(*p*-bromophenyl)nitrosoethylene. The structure and the lowest energy conformations of this nitrosoalkene have been previously investigated [4] at the same level of theory, being the *s-trans* conformer found to be more stable than the *s-cis* conformer ($\Delta E = 5.6$ kJ/mol). It was also found an increase in the electrostatic moment from *s-cis* (2.16 D) to *s-trans* (2.80 D), suggesting a preference for the *s-trans*-conformer in polar media [7].

The energy barriers corresponding to the transitions states, and the synchronicities associated with the formation of the corresponding products are reported in Table 2.

The results include zero-point-energy (ZPE) and counterpoise basis set superposition error (BSSE) corrections. The results demonstrate that the barriers associated with the reactions between indole and its derivatives with the considered nitrosoalkene are very similar, pointing to a process occurring in a concerted way, in all cases through an *exo*-approach. Moreover, the barriers associated with the experimentally observed regiochemistry are lower than those associated with the opposite one (see Table 2). The optimized geometries of the relevant transition structures are presented in Fig. 1.

DFT calculations have also been carried to determine the HOMO and LUMO energies of the 1-(*p*-bromophenyl)nitrosoethylene and indole (Table 3). The results suggest the presence of the $\text{LUMO}_{\text{nitrosoalkene}}/\text{HOMO}_{\text{indole}}$ in the dominant interaction and consequently an inverse-electron-demand Diels–Alder reaction.

The energy barriers associated with the reactions between 1-(*p*-bromophenyl)nitrosoethylene and indole and its derivatives are similar to those observed for the reaction between the nitrosoalkene and pyrrole, which was found to take place by a different reaction pathway [7]. In order to understand the different reactivity of indole and pyrrole towards this nitrosoalkene, the structure and energy of the theoretical Diels–Alder cycloadducts formed in each case were investigated. The same approach was also used to understand the regiochemistry observed in the Diels–Alder cycloaddition involving nitrosoalkene **5a** and the indole derivatives. The cycloadditions of the nitrosoalkene with

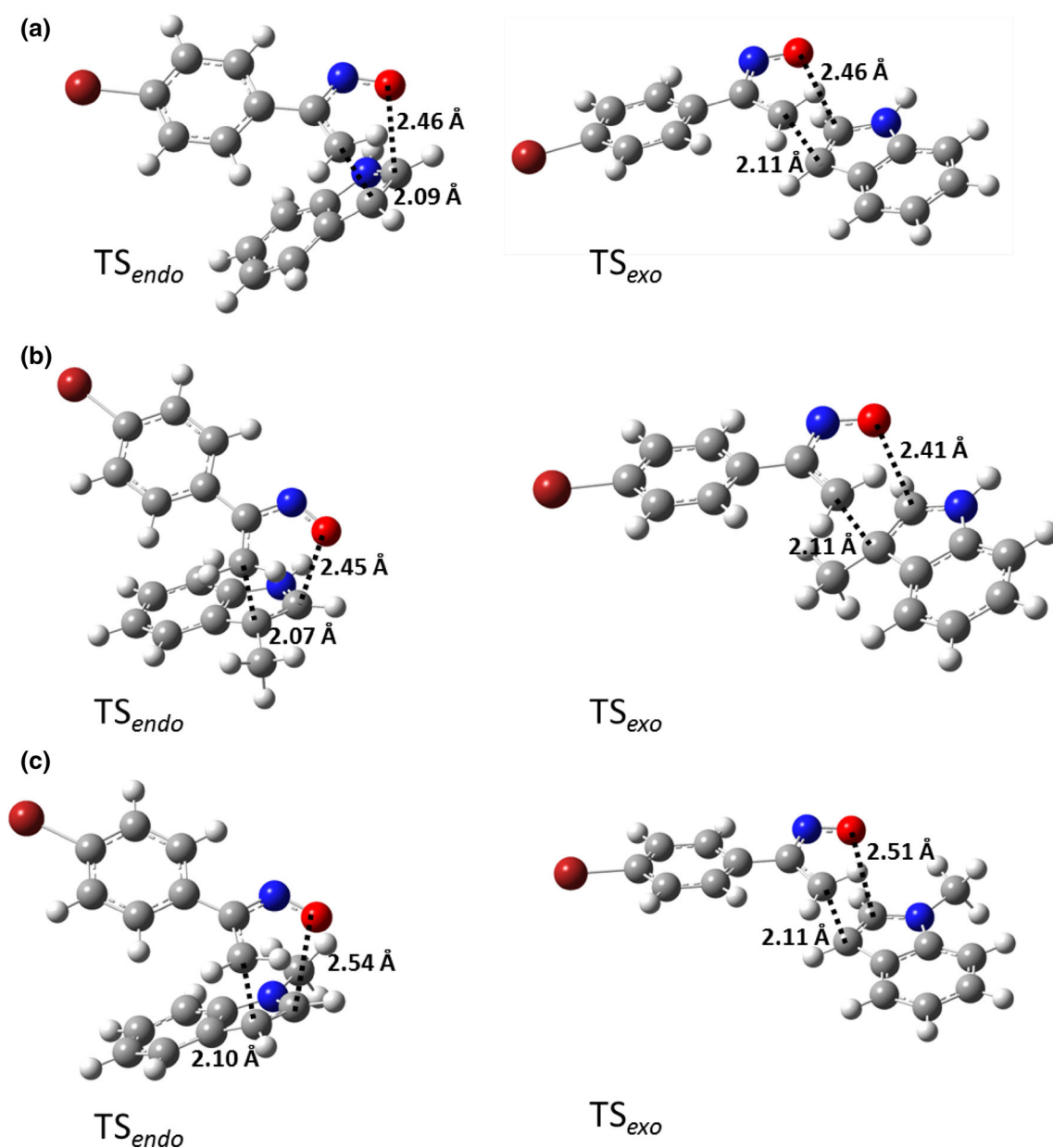


Fig. 1 Optimized geometries (B3LYP/6-31G(d,p) level) of the most relevant transition state structures found for the reaction of 1-(*p*-bromophenyl)nitrosoethylene (**5a**) with **a** indole, **b** 3-methylindole, and **c** 1-methylindole

Table 3 Frontier orbital energy differences (eV) for the HOMO–LUMO for the reaction between **5a** and indole at B3LYP/6-31G(d,p) level of theory

	<i>E</i> /eV		HOMO–LUMO pair	ΔE /eV
	HOMO	LUMO		
Indole	−5.42	−0.09	HOMO _{indole} –LUMO _{5a}	2.34
5a	−6.3	−3.08	HOMO _{5a} –LUMO _{indole}	6.21

indole was selected as the model reaction. Figure 2 represents schematically the energy difference between the reactants and products in each case. The results

demonstrate that, in the case of the indole, the energy difference between reactants and products clearly favors the regiochemistry observed experimentally (a).

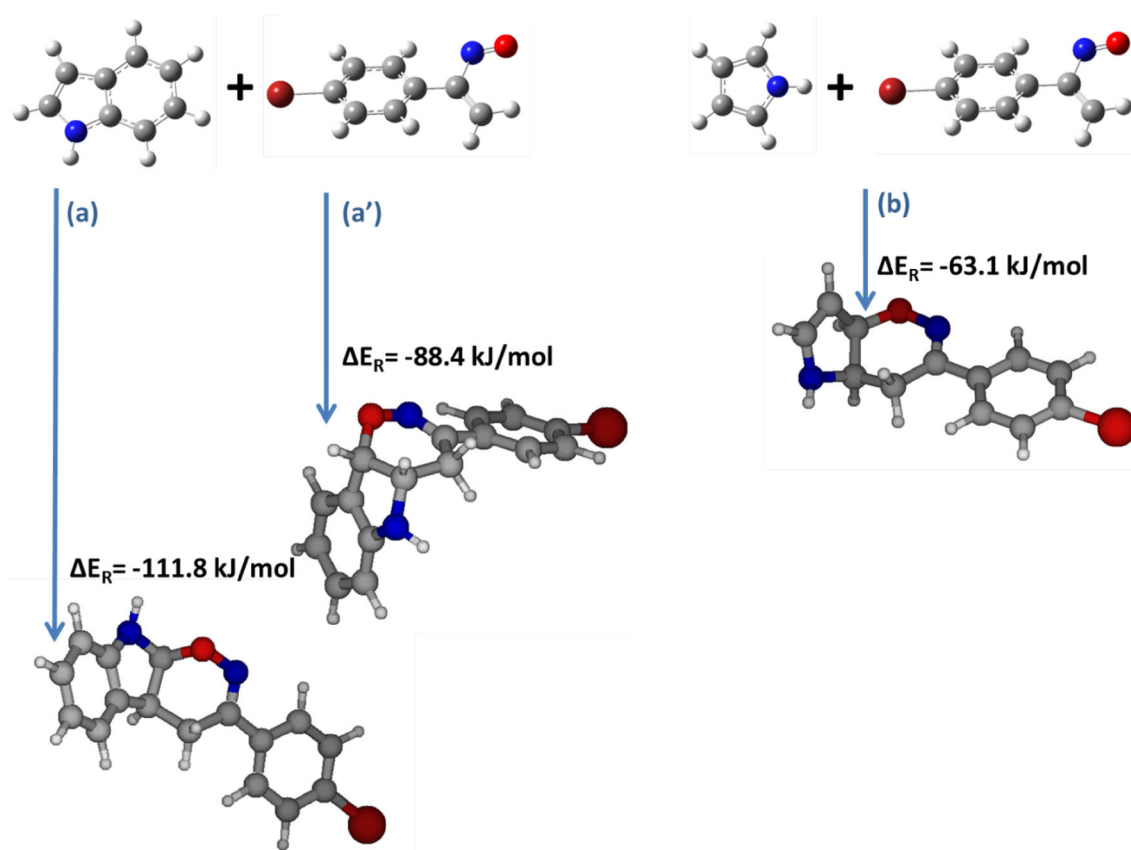


Fig. 2 Schematic representation of the B3LYP/6-31G(d,p) energy difference (ΔE_R , kJ/mol) between reactants and the hypothetically formed cycloadduct for the reactions between indole and 1-(*p*-bromophenyl)nitrosoethylene with the regiochemistry observed

experimentally (a) and with the opposite regiochemistry (a'). Reaction **b** corresponds to the hypothetical formation of the cycloadduct resulting from the addition of pyrrole to 1-(*p*-bromophenyl)nitrosoethylene

Additionally, the comparison between the reactions involving indole and pyrrole clearly suggests that the Diels–Alder reaction is privileged in the case of indole.

Conclusion

The results on the reactivity of 1-arylnitrosoethylene toward indole, 1-methylindole, and 3-methylindole are consistent with a process involving hetero-Diels–Alder reactions, the same reactivity observed in the reaction of indole with ethyl nitrosoacrylate. Thus, indole and 1-methylindole react with 1-arylnitrosoethylene affording hetero-Diels–Alder cycloadducts, followed by 1,2-oxazine ring-opening reaction to give 3-alkylated indoles. The reaction with 3-methylindole gave the corresponding cycloadduct since aromatization of the pyrrole unit is precluded.

These results are in contrast with the previously observed chemical behaviour of 1-arylnitrosoethylene in the reaction with pyrrole, which proceeds via a conjugate

addition followed by a 1,5-sigmatropic hydrogen shift leading to a mixture of isomeric oximes.

Quantum chemical calculations, at the DFT level, were carried out corroborating the mechanistic proposal. The energy barriers associated with the reactions between 1-(*p*-bromophenyl)nitrosoethylene and indole and its derivatives are similar to those observed for the reaction between the nitrosoalkene and pyrrole. However, the calculated energy of the theoretical Diels–Alder cycloadducts involving indole and pyrrole clearly suggests that the Diels–Alder reaction is privileged in the case of indole. Furthermore, in the case of the indole, the energy difference between reactants and products clearly favors the regiochemistry observed experimentally.

Experimental

^1H NMR spectra were recorded on an instrument operating at 400 MHz. ^{13}C NMR spectra were recorded on an instrument operating at 100 MHz. The solvent was

hexadeuterodimethyl sulfoxide (DMSO- d_6) or deuterium chloroform (CDCl₃). Chemical shifts are expressed in parts per million relative to internal TMS, and coupling constants (J) are in Hz. Infrared spectra (IR) were recorded on a Fourier transform spectrometer. High-resolution mass spectra (HRMS) were obtained on an electrospray (ESI) TOF or electron impact (EI) TOF mass spectrometer. Melting points were determined in open glass capillaries. Thin-layer chromatography (TLC) analyses were performed using precoated silica gel plates. Flash column chromatography was performed with silica gel 60 as the stationary phase. 2-Bromo-1-(*p*-bromophenyl)ethanone oxime (**12a**), 2-bromo-1-phenylethanone oxime (**12b**), 2-bromo-1-(*p*-nitrophenyl)ethanone oxime (**12c**), and 2-bromo-1-(*p*-methoxyphenyl)ethanone oxime (**12d**) [14–16] were prepared as described in the literature.

General procedure

Indole, 1-methylindole, or 3-methylindole (1.36 mmol) and oximes **12** (0.68 mmol) were added to a suspension of Na₂CO₃ (3.4 mmol) in 20 cm³ dichloromethane. The reaction mixture was stirred at room temperature for the time indicated in each case. The reaction was monitored by TLC. Upon completion, the mixture was filtered through a Celite pad, which was washed with dichloromethane. The solvent was evaporated, and the product was purified by flash chromatography.

Compounds 13a, 14a, and 15a

Obtained from 200 mg oxime **12a** (0.68 mmol) and 159 mg indole (1.36 mmol) following the general procedure (reaction time 17 h). Purification of the crude product by flash chromatography (ethyl acetate/hexane, 1:3), gave, in order of elution, **13a** as a white solid (52.9 mg, 24 %), **14a** as a white solid (29.1 mg, 16 %), and **15a** as a white solid (43.7 mg, 24 %).

(E)-1-(*p*-Bromophenyl)-2-(1*H*-indol-3-yl)ethanone oxime (**13a**, C₁₆H₁₃BrN₂O)

Mp.: 155.3–156.8 °C; ¹H NMR (400 MHz, DMSO- d_6): δ = 4.18 (s, 2H), 6.93–6.97 (m, 1H), 7.02–7.05 (m, 2H), 7.29 (d, 1H, J = 8.0 Hz), 7.47–7.50 (m, 2H), 7.59–7.63 (m, 2H), 10.77 (br s, 1H), 11.57 (s, 1H) ppm; ¹³C NMR (100 MHz, DMSO- d_6): δ = 20.5, 109.2, 111.3, 118.3, 118.4, 121.0, 121.8, 123.5, 126.8, 128.1, 131.1, 135.3, 136.0, 154.4 ppm; IR (KBr): $\bar{\nu}$ = 742, 791, 924, 956, 966, 1315, 1456, 1489, 3240, 3406, 3417 cm⁻¹; HRMS (ESI-TOF): m/z calcd. for C₁₆H₁₄BrN₂O 329.02840 [M + H⁺], found 329.02831.

(E)-1-(*p*-Bromophenyl)-2-[3-[(*E*)-2-(*p*-bromophenyl)-2-(hydroxyimino)ethyl]-1*H*-indol-1-yl]ethanone oxime (**14a**, C₂₄H₁₉Br₂N₃O₂)

Mp.: 170.4–171.9 °C; ¹H NMR (400 MHz, DMSO- d_6): δ = 4.09 (s, 2H), 5.44 (s, 2H), 6.95–6.97 (m, 1H), 7.07–7.09 (m, 2H), 7.32–7.34 (m, 3H), 7.39 (d, 2H, J = 8.4 Hz), 7.45 (d, 2H, J = 8.4 Hz), 7.52–7.54 (m, 3H), 11.57 (s, 1H), 12.10 (s, 1H) ppm; ¹³C NMR (100 MHz, DMSO- d_6): δ = 20.4, 38.7, 109.2, 109.4, 118.8, 121.4, 121.8, 122.2, 127.2, 127.5, 128.0, 128.3, 131.0, 131.1, 133.4, 135.1, 135.8, 152.0, 154.0 ppm; IR (KBr): $\bar{\nu}$ = 746, 960, 980, 1250, 1444, 1464, 1491, 1587, 3215, 3244 cm⁻¹; HRMS (ESI-TOF): m/z calcd. for C₂₄H₂₀Br₂N₃O₂ 539.99168 [M + H⁺], found 539.99149.

(E)-1-(*p*-Bromophenyl)-2-[1-[(*Z*)-2-(4-bromophenyl)-2-(hydroxyimino)ethyl]-1*H*-indol-3-yl]ethanone oxime (**15a**, C₂₄H₁₉Br₂N₃O₂)

Mp.: 186.2–187.9 °C; ¹H NMR (400 MHz, DMSO- d_6): δ = 4.10 (s, 2H), 5.17 (s, 2H), 6.95–6.99 (m, 2H), 7.07–7.11 (m, 1H), 7.25–7.27 (m, 2H), 7.40 (d, 3H, J = 8.4 Hz), 7.46–7.49 (m, 2H), 7.53–7.58 (m, 3H), 11.33 (s, 1H), 11.58 (s, 1H) ppm; ¹³C NMR (100 MHz, DMSO- d_6): δ = 20.4, 49.0, 109.3, 109.9, 118.7, 121.3, 121.8, 122.0, 126.9, 127.4, 128.0, 130.2, 130.5, 130.7, 131.1, 135.1, 136.1, 150.8, 154.1 ppm; IR (KBr): $\bar{\nu}$ = 737, 827, 943, 991, 1076, 1392, 1466, 1487, 1585, 3247 cm⁻¹; HRMS (ESI-TOF): m/z calcd. for C₂₄H₂₀Br₂N₃O₂ 539.99168 [M + H⁺], found 539.99148.

Compounds 13b, 14b, and 15b

Obtained from 146 mg oxime **12b** (0.68 mmol) and 159 mg indole (1.36 mmol) following the general procedure (reaction time, 46 h). Purification of the crude product by flash chromatography (ethyl acetate/hexane, 1:3), gave, in order of elution, **13b** as a yellow solid (45.9 mg, 27 %), **14b** as a white solid (18.2 mg, 14 %), and **15b** as a white solid (36.5 mg, 28 %).

(E)-2-(1*H*-Indol-3-yl)-1-phenylethanone oxime (**13b**, C₁₆H₁₄N₂O)

Mp.: 163.8–164.9 °C; ¹H NMR (400 MHz, DMSO- d_6): δ = 4.21 (s, 2H), 6.97 (t, 1H, J = 7.2 Hz), 7.04–7.07 (m, 2H), 7.28–7.33 (m, 4H), 7.64 (d, 1H, J = 7.6 Hz), 7.69–7.71 (m, 2H), 10.77 (br s, 1H), 11.44 (s, 1H) ppm; ¹³C NMR (100 MHz, DMSO- d_6): δ = 20.7, 109.5, 111.3, 118.3, 118.5, 120.9, 123.5, 126.1, 126.9, 128.2, 128.4, 136.0, 136.1, 155.2 ppm; IR (KBr): $\bar{\nu}$ = 688, 742, 924, 964, 1074, 1223, 1317, 1456, 3060, 3242, 3400 cm⁻¹; HRMS (ESI-TOF): m/z calcd. for C₁₆H₁₅N₂O 251.11789 [M + H⁺], found 251.11779.

(*E*)-2-[1-[(*Z*)-2-(Hydroxyimino)-2-phenylethyl]-1*H*-indol-3-yl]-1-phenylethanone oxime (**14b**, C₂₄H₂₁N₃O)
Mp.: 150.9–152.8 °C; IR (¹H NMR (400 MHz, DMSO-*d*₆): δ = 4.09 (s, 2H), 5.44 (s, 2H), 6.96 (t, 1H, *J* = 7.6 Hz), 7.06–7.09 (m, 2H), 7.17–7.29 (m, 6H), 7.39 (d, 1H, *J* = 8.4 Hz), 7.47–7.49 (m, 2H), 7.55–7.60 (m, 3H), 11.41 (s, 1H), 11.96 (s, 1H) ppm; ¹³C NMR (100 MHz, DMSO-*d*₆): δ = 20.7, 38.8, 109.4, 109.5, 118.7, 118.8, 121.3, 126.0, 126.3, 127.3, 127.4, 128.1, 128.2, 128.4, 128.8, 134.3, 135.9, 136.1, 152.8, 154.9 ppm; (KBr): $\bar{\nu}$ = 694, 756, 918, 966, 1319, 1468, 3244 cm⁻¹; HRMS (ESI-TOF): *m/z* calcd. for C₂₄H₂₂N₃O₂ 384.17065 [M + H⁺], found 384.17063.

(*E*)-2-[3-[(*E*)-2-(Hydroxyimino)-2-phenylethyl]-1*H*-indol-1-yl]-1-phenylethanone oxime (**15b**, C₂₄H₂₁N₃O₂)
Mp.: 171.2–172.4 °C; ¹H NMR (400 MHz, DMSO-*d*₆): δ = 4.10 (s, 2H), 5.15 (s, 2H), 6.96–6.99 (m, 2H), 7.06–7.10 (m, 1H), 7.22–7.25 (m, 2H), 7.29–7.33 (m, 5H), 7.41 (d, 2H, *J* = 8.0 Hz), 7.58–7.62 (m, 3H), 11.14 (s, 1H), 11.41 (s, 1H) ppm; ¹³C NMR (100 MHz, DMSO-*d*₆): δ = 20.6, 49.2, 109.4, 110.0, 118.6, 118.7, 121.2, 125.9, 126.9, 127.5, 127.7, 128.0, 128.2, 128.4, 128.6, 131.6, 136.0, 136.2, 151.6, 154.9 ppm; IR (KBr): $\bar{\nu}$ = 696, 741, 766, 949, 989, 1308, 1435, 1466, 3248 cm⁻¹; HRMS (ESI-TOF): *m/z* calcd. for C₂₄H₂₂N₃O₂ 384.17065 [M + H⁺], found 384.17054.

(*E*)-1-(*p*-Bromophenyl)-2-(1-methyl-1*H*-indol-3-yl)ethanone oxime (**16a**, C₁₇H₁₅BrN₂O)
Obtained from 200 mg oxime **12a** (0.68 mmol) and 0.170 cm³ 1-methylindole (1.36 mmol) following the general procedure (reaction time, 16 h). Purification of the crude product by crystallization with dichloromethane, gave **16a** as a white solid (194 mg, 83 %). Mp.: 173.4–174.3 °C; ¹H NMR (400 MHz, DMSO-*d*₆): δ = 3.66 (s, 3H), 4.17 (s, 2H), 6.97–7.01 (m, 2H), 7.11 (t, 1H, *J* = 7.2 Hz), 7.32 (d, 1H, *J* = 8.4 Hz), 7.50 (d, 2H, *J* = 8.8 Hz), 7.61–7.64 (m, 3H), 11.58 (s, 1H) ppm; ¹³C NMR (100 MHz, DMSO-*d*₆): δ = 20.4, 32.2, 108.5, 109.5, 118.4, 118.6, 121.1, 121.8, 127.2, 127.7, 128.1, 131.2, 135.2, 136.4, 154.3 ppm; IR (KBr): $\bar{\nu}$ = 740, 827, 922, 949, 1059, 1313, 1333, 1485, 1658, 2912, 3059, 3217 cm⁻¹; HRMS (ESI-TOF): *m/z* calcd. for C₁₇H₁₆BrN₂O 343.04405 [M + H⁺], found 343.04413.

(*E*)-1-(*p*-Nitrophenyl)-2-(1-methyl-1*H*-indol-3-yl)ethanone oxime (**16b**, C₁₇H₁₅N₃O₃)
Obtained from 176 mg oxime **12c** (0.68 mmol) and 0.170 cm³ 1-methylindole (1.36 mmol) as described in general procedure method (reaction time, 25 h). Purification of the crude product by crystallization with diethyl ether/petroleum ether, gave **16b** obtained as a yellow solid

(187 mg, 89 %). Mp.: 179.6–180.5 °C; ¹H NMR (400 MHz, DMSO-*d*₆): δ = 3.66 (s, 3H), 4.25 (s, 2H), 6.99–7.02 (m, 1H), 7.05 (s, 1H), 7.10–7.14 (m, 1H), 7.33 (d, 1H, *J* = 8.0 Hz), 7.62 (d, 1H, *J* = 8.0 Hz), 7.94–7.96 (m, 2H), 8.15–8.17 (m, 2H), 12.02 (s, 1H) ppm; ¹³C NMR (100 MHz, DMSO-*d*₆): δ 20.4, 32.2, 108.0, 109.6, 118.5, 118.6, 121.2, 123.5, 127.1, 127.8, 136.4, 142.3, 147.1, 154.0 ppm; IR (ATR): $\bar{\nu}$ = 730, 855, 944, 1335, 1513, 2909, 3049, 3225 cm⁻¹; HRMS (EI-TOF): *m/z* calcd. for C₁₇H₁₅N₃O₃ 309.1113 [M⁺], found 309.1108.

(*E*)-1-(*p*-Methoxyphenyl)-2-(1-methyl-1*H*-indol-3-yl)ethanone oxime (**16c**, C₁₈H₁₈N₂O₂)
Obtained from 166 mg oxime **12d** (0.68 mmol) and 0.170 cm³ 1-methylindole (1.36 mmol) as described in general procedure method (reaction time, 24 h). Purification of the crude product by flash chromatography (ethyl acetate/hexane, 1:3), gave **16c** obtained as a white solid (148 mg, 74 %). Mp.: 110.8–112.6 °C; ¹H NMR (400 MHz, CDCl₃): δ = 3.64 (s, 3H), 3.76 (s, 3H), 4.25 (s, 2H), 6.81–6.83 (m, 3H), 7.10–7.12 (m, 1H), 7.19–7.26 (m, 6H), 7.60–7.64 (m, 2H), 7.68 (d, 1H, *J* = 7.6 Hz), 9.17 (br s, 1H) ppm; ¹³C NMR (100 MHz, CDCl₃): δ = 22.2, 32.7, 55.3, 109.1, 109.2, 113.9, 118.9, 121.6, 127.3, 127.7, 127.9, 128.3, 137.0, 157.6, 160.5 ppm; IR (ATR): $\bar{\nu}$ = 747, 953, 1175, 1254, 1513, 1599, 2927, 3247 cm⁻¹; HRMS (EI-TOF): *m/z* calcd. for C₁₈H₁₈N₂O₂ 294.1368 [M⁺], found 294.1378.

3-(*p*-Bromophenyl)-4*a*-methyl-4,4*a*,9,9*a*-tetrahydro[1, 2]oxazine[6,5-*b*]indole (**17a**, C₁₇H₁₅BrN₂O)
Obtained from 200 mg oxime **12a** (0.68 mmol) and 178 mg 3-methylindole (1.36 mmol) as described in general procedure method (reaction time, 91 h). Purification of the crude product by flash chromatography (ethyl acetate/hexane, 1:3), gave **17a** as a beige solid (168 mg, 72 %). Mp.: 153.1–153.8 °C; ¹H NMR (400 MHz, CDCl₃): δ = 1.53 (s, 3H), 2.68 (d, 1H, *J* = 14.4 Hz), 2.99 (d, 1H, *J* = 14.4 Hz), 4.80 (br s, 1H), 5.40 (s, 1H), 6.52 (d, 1H, *J* = 7.6 Hz), 6.65 (t, 1H, *J* = 7.6 Hz), 6.96–7.00 (m, 2H), 7.38 (d, 2H, *J* = 8.4 Hz), 7.45 (d, 2H, *J* = 8.4 Hz) ppm; ¹³C NMR (100 MHz, CDCl₃): δ = 26.8, 33.0, 48.5, 96.4, 108.2, 119.0, 122.1, 124.8, 127.5, 128.4, 131.8, 132.4, 133.4, 148.4, 169.4 ppm; IR (KBr): $\bar{\nu}$ = 746, 829, 874, 1072, 1469, 1487, 1610 cm⁻¹; HRMS (ESI-TOF): *m/z* calcd. for C₁₇H₁₆BrN₂O 343.04405 [M + H⁺], found 343.04397.

3-(*p*-Nitrophenyl)-4*a*-methyl-4,4*a*,9,9*a*-tetrahydro[1, 2]oxazine[6,5-*b*]indole (**17b**, C₁₇H₁₅N₃O₃)
Obtained from 176 mg oxime **12c** (0.68 mmol) and 178 mg 3-methylindole (1.36 mmol) as described in general procedure method (reaction time, 17 h 30 min). Purification of the crude product by flash chromatography

(ethyl acetate/hexane, 1:3), gave **17b** obtained as a yellow solid (177 mg, 84 %). M.p.: 160.5–161.3 °C; ^1H NMR (400 MHz, CDCl_3): δ = 1.57 (s, 3H), 2.73 (d, 1H, J = 14.4 Hz), 3.07 (d, 1H, J = 14.4 Hz), 4.84 (br s, 1H), 5.47 (d, 1H, J = 1.2 Hz), 6.54–6.56 (m, 1H), 6.64–6.68 (m, 1H), 6.97–7.01 (m, 2H), 7.66–7.69 (m, 2H), 8.16–8.19 (m, 2H) ppm; ^{13}C NMR (100 MHz, CDCl_3): δ = 26.8, 33.1, 48.5, 96.6, 108.3, 119.2, 122.0, 123.8, 126.9, 128.5, 132.1, 140.4, 148.2, 148.8, 168.2 ppm; IR (ATR): $\bar{\nu}$ = 748, 853, 1116, 1351, 1518, 1563, 1606 cm^{-1} ; HRMS (EI-TOF): m/z calcd. for $\text{C}_{17}\text{H}_{15}\text{N}_3\text{O}_3$ 309.1113 [M^+], found 309.1117.

3-(p-Methoxyphenyl)-4a-methyl-4,4a,9,9a-tetrahydro[1,2]oxazine[6,5-b]indole (17c, $\text{C}_{18}\text{H}_{18}\text{N}_2\text{O}_2$)

Obtained from 166 mg oxime **12d** (0.68 mmol) and 178 mg 3-methylindole (1.36 mmol) as described in general procedure method (reaction time, 17 h 30 min). Purification of the crude product by flash chromatography (ethyl acetate/hexane, 1:3), gave **17c** obtained as a white fluffy solid (68 mg, 34 %). M.p.: 39.1–40.6 °C; ^1H NMR (400 MHz, CDCl_3): δ = 1.51 (s, 3H), 2.69 (d, 1H, J = 14.2 Hz), 3.00 (d, 1H, J = 14.2 Hz), 3.79 (s, 3H), 4.77 (br s, 1H), 5.36 (s, 1H), 6.53 (d, 1H, J = 8.0 Hz), 6.66 (td, 1H, J = 7.4 Hz, 0.6 Hz), 6.82–6.86 (m, 2H), 6.98 (td, 1H, J = 7.7 Hz, 1.1 Hz), 7.02 (d, 1H, J = 7.4 Hz), 7.49–7.53 (m, 2H) ppm; ^{13}C NMR (100 MHz, CDCl_3): δ = 26.8, 33.0, 48.5, 55.3, 96.3, 108.1, 113.9, 118.9, 122.2, 126.9, 127.5, 128.2, 132.8, 148.5, 161.4, 169.9 ppm; IR (ATR): $\bar{\nu}$ = 741, 827, 1176, 1248, 1513, 1606 cm^{-1} ; HRMS (EI-TOF): m/z calcd. for $\text{C}_{18}\text{H}_{18}\text{N}_2\text{O}_2$ 294.1368 [M^+], found 294.1377.

Acknowledgments Thanks are due to Coimbra Chemistry Centre (CQC), supported by the Portuguese Agency for Scientific Research, “Fundação para a Ciência e a Tecnologia” (FCT), through Project No. 007630 UID/QUI/00313/2013, co-funded by COMPETE2020-UE. Sandra C. C. Nunes and Susana M. M. Lopes also acknowledge FCT for postdoctoral research grants SFRH/BPD/71683/2010, SFRH/BPD/84413/2012, respectively. We acknowledge the UC-NMR facility for obtaining the NMR data (<http://www.nmrccc.uc.pt>).

References

1. Gilchrist TL (1983) *Chem Soc Rev* 12:53
2. Lyapkalo IM, Ioffe I (1998) *Russ Chem Rev* 67:467
3. Reissig H-U, Zimmer R (2006) 1-Nitrosoalkenes. In: Molander GA (ed) *Science of synthesis*, vol 33. Thieme, Stuttgart, Germany
4. Gilchrist TL, Roberts TG (1983) *J Chem Soc Perkin Trans 1*:1283
5. Lopes SMM, Lemos A, Pinho e Melo TMVD (2010) *Tetrahedron Lett* 51:6756
6. Lopes SMM, Palacios F, Lemos A, Pinho e Melo TMVD (2011) *Tetrahedron* 67:8902
7. Nunes SCC, Lopes SCC, Gomes CSB, Lemos A, Pais AACC, Pinho e Melo TMVD (2014) *J Org Chem* 79:10456
8. Clarke SJ, Gilchrist TL, Lemos A, Roberts TG (1991) *Tetrahedron* 47:5615
9. Lopes SMM, Brigas AF, Palacios F, Lemos A, Pinho e Melo TMVD (2012) *Eur J Org Chem* 2012(11):2152–2160
10. Schmidt MW, Baldrige KK, Boatz JA, Elbert ST, Gordon MS, Jensen JH, Koseki S, Matsunaga N, Nguyen KA, Su SJ, Windus TL, Dupuis M, Montgomery JA (1993) *J Comput Chem* 14:1347
11. Becke AD (1988) *Phys Rev A* 38:3098
12. Becke AD (1993) *J Chem Phys* 98:5648
13. Lee CT, Yang WT, Parr RG (1988) *Phys Rev B* 37:785
14. Hartung J, Schwarz M (2002) *Org Synth* 79:228
15. Blumbergs P, Thanawalla CB, Ash AB, Lieske CN, Steinberg GM (1971) *J Org Chem* 36:2023
16. Davies DE, Gilchrist TL, Roberts TG (1983) *J Chem Soc Perkin Trans 1*:1275